

## Pinning Mode Resonances of 2D Electron Stripe Phases: Effect of an In-Plane Magnetic Field

Han Zhu,<sup>1,2</sup> G. Sambandamurthy,<sup>2,3</sup> L. W. Engel,<sup>2</sup> D. C. Tsui,<sup>3</sup> L. N. Pfeiffer,<sup>4</sup> and K. W. West<sup>4</sup>

<sup>1</sup>*Department of Physics, Princeton University, Princeton, New Jersey 08544, USA*

<sup>2</sup>*National High Magnetic Field Laboratory, Tallahassee, Florida 32310, USA*

<sup>3</sup>*Department of Electrical Engineering, Princeton University, Princeton, New Jersey 08544, USA*

<sup>4</sup>*Bell Laboratories, Alcatel-Lucent Technologies, Murray Hill, New Jersey 07974, USA*

(Received 20 October 2008; published 31 March 2009)

We study the anisotropic pinning-mode resonances in the rf conductivity spectra of the stripe phase of 2D electron systems around a Landau level filling of  $9/2$ , in the presence of an in-plane magnetic field  $B_{ip}$ . The polarization along which the resonance is observed switches as  $B_{ip}$  is applied, consistent with the reorientation of the stripes. The resonance frequency, a measure of the pinning interaction between the 2D electron systems and disorder, increases with  $B_{ip}$ . The magnitude of this increase indicates that disorder interaction is playing an important role in determining the stripe orientation.

DOI: 10.1103/PhysRevLett.102.136804

PACS numbers: 73.43.-f, 32.30.Bv, 73.20.Qt

Many systems in nature exhibit phases with spontaneous spatial modulation of charge density in a stripe pattern. Such stripe phases exist in extremely low disorder two-dimensional electron systems (2DES) hosted in a high magnetic field, for Landau level fillings near  $\nu = 9/2, 11/2, 13/2, \dots$ . The stripe phases are manifested in dc transport [1,2] by strong anisotropy below about 150 mK, with smaller and larger diagonal resistivities, respectively, along orthogonal “easy” and “hard” directions that are fixed in the semiconductor host lattice. Early theoretical work [3,4] on 2DES near these fillings predicted the stripe phases even before the experiments and described them as unidirectional charge density waves. Later theoretical pictures were based on analogy with liquid crystals and included quantum Hall smectics [5], as well as quantum Hall nematic states, with local smectic order but long range orientational order [6,7]. Yet another proposed state for the stripes [8–11] is a highly anisotropic rectangular lattice, which is referred to as the “stripe crystal.”

This Letter focuses on the symmetry breaking which determines the orientation of the stripes in the sample plane. In the absence of an in-plane magnetic field, the mechanism is still not understood, despite a great deal of attention [12–15]: For the density and quantum well width of the samples studied in this Letter, the easy direction, along which the stripes are expected to lie, is in the [110] direction of the GaAs host lattice. When in-plane magnetic field  $B_{ip}$  is present, it acts as a symmetry-breaking field and can interchange the hard and easy axes in the sample, as demonstrated by studies of dc transport [13–20]. This Letter shows that disorder, though small enough in these samples not to destroy the anisotropy, plays an important role in this symmetry breaking and, further, that the disorder interaction *depends on*  $B_{ip}$ .

The disorder interaction is accessed from the recently discovered [21] radio frequency “pinning mode” of the

stripe phases. This mode is a collective oscillation of correlated pieces of the electronic phase within the potential of pinning impurities, and its frequency is a measure of the average potential energy of a carrier [22–24] in the pinning disorder. The pinning mode appears as a striking resonance in the spectrum of stripe-phase diagonal conductivity along the hard direction, nominally perpendicular to the stripes, though the spectrum is essentially flat in the easy direction, parallel to the stripes. Similar (but isotropic) resonances have been observed in many high-magnetic-field electron solids, including the Wigner crystal phases, found at the high-magnetic-field termination [25,26] of the fractional quantum Hall series and at the outer edges of integer quantum Hall plateaus [27], and also the bubble phases [28,29], which exist in regions of  $\nu$  immediately adjacent to the stripes. Pinning modes of the stripe phase have also been studied theoretically [9,30].

A theoretical framework [31,32], which does not include disorder, obtains a per-electron energy difference between stripe orientations perpendicular and parallel to  $B_{ip}$ . This energy, denoted  $E_A$  [31,32], is found from the effect of  $B_{ip}$  on the wave function in the direction ( $z$ ) perpendicular to the 2D plane in a finite-thickness 2DES, for the stripe in a unidirectional charge density wave state. This anisotropy energy  $E_A$  favors the stripes being perpendicular to  $B_{ip}$ , in accord with dc transport studies [13–19], in which, for most of the sample surveyed, switching the stripe direction in the sample at least occurs for  $B_{ip}$  applied in the original (i.e.,  $B_{ip} = 0$ ) easy direction. Not addressed in that theoretical framework are experimental results for  $B_{ip}$  applied perpendicular to the original  $B_{ip} = 0$  easy axis, which show that dc resistances along the sample axes can approach each other [15–18] and even cross over in some cases [15,16], leaving the axis of lower dc resistance parallel to  $B_{ip}$ .

In this Letter, we examine the dependence of the pinning resonances of the stripe phases on  $B_{ip}$ . We find  $B_{ip}$  to

switch the axis along which the resonance is observed, much as it switches the hard and easy axes in the dc transport experiments [13–20]. Switching occurs for  $B_{ip}$  applied along either the original hard or original easy axis. For  $B_{ip}$  near the switching point, resonances appear for polarizations in both directions, suggesting that coexisting, perpendicularly oriented domains are present as the switching occurs. A unique feature of the present experiments is the information on pinning strength provided by the measured resonance frequency  $f_{pk}$ , which we find increases vs  $B_{ip}$ , at different rates depending on the axis in which  $B_{ip}$  is applied. We find that the change due to  $B_{ip}$  of the average binding energy of carriers in the disorder potential is comparable to the theoretically predicted [31,32]  $B_{ip}$ -induced anisotropy energy. The results imply that the disorder-carrier interaction is  $B_{ip}$ -dependent and plays an important role in determining stripe orientation, even when significant  $B_{ip}$  is applied.

The sample wafer is a 30 nm GaAs/ $Al_xGa_{1-x}$ As quantum well, with density  $2.7 \times 10^{11}/\text{cm}^2$  and mobility  $29 \times 10^6 \text{ cm}^2/\text{V s}$  at 0.3 K. As in earlier work [21,25,27,28], we evaporated a coplanar wave guide (CPW) transmission line onto the sample surface. The CPW consists of a driven, straight center line separated from grounded planes on either side by a slot of width  $w = 78 \mu\text{m}$ . The line has length  $l \sim 4 \text{ mm}$ , and its characteristic impedance  $Z_0 = 50 \Omega$  when the 2DES conductivity is small. From the absorption of the signal by the 2DES, the real part of the 2DES diagonal conductivity in direction  $j$  is calculated as  $\text{Re}[\sigma_{jj}(f)] = (w/2lZ_0) \ln(P_t/P_0)$ , where  $P_t$  is the transmitted power, normalized by  $P_0$ , the power transmitted at zero  $\sigma_{jj}$ . At the measuring frequencies, the rf electric field  $E_{rf}$  produced by the CPW is well-polarized perpendicular to the propagation direction. In order to measure conductivities  $\sigma_{xx}$  and  $\sigma_{yy}$  along orthogonal crystal axes of the sample, we present data from two adjacent pieces of the same wafer and patterned CPWs along perpendicular axes.  $\hat{x}$  denotes the GaAs crystal axis  $[1\bar{1}0]$ , which for the present samples is the dc hard direction at  $\nu = 9/2$  in zero  $B_{ip}$ .  $\hat{y}$  is the crystal axis  $[110]$ , the zero- $B_{ip}$  dc easy direction. Sample 1 has  $E_{rf}$  along  $\hat{x}$ ; sample 2 has  $E_{rf}$  along  $\hat{y}$ .

We applied  $B_{ip}$  by tilting the sample in a rotator with low-loss, broadband, flexible transmission lines. The temperature of all measurements reported here is around 40 mK. The rotation angle  $\theta$  is calculated from the magnetic fields of prominent quantum Hall states. From perpendicular field  $B_{\perp}$ ,  $B_{ip} = B_{\perp} \tan\theta$ .  $B_{ip}$  can also be directed to be along either  $\hat{x}$  or  $\hat{y}$  (in separate cooldowns), so we present data from a total of four combinations of  $E_{rf}$  and  $B_{ip}$  directions.

Figure 1 shows spectra of the real diagonal conductivities  $\text{Re}(\sigma_{xx})$  and  $\text{Re}(\sigma_{yy})$  at filling factor  $\nu = 9/2$ , with  $B_{ip}$  applied along  $\hat{y}$ , parallel to the stripe orientation at zero  $B_{ip}$ . For reference, Fig. 1(a) shows spectra taken with

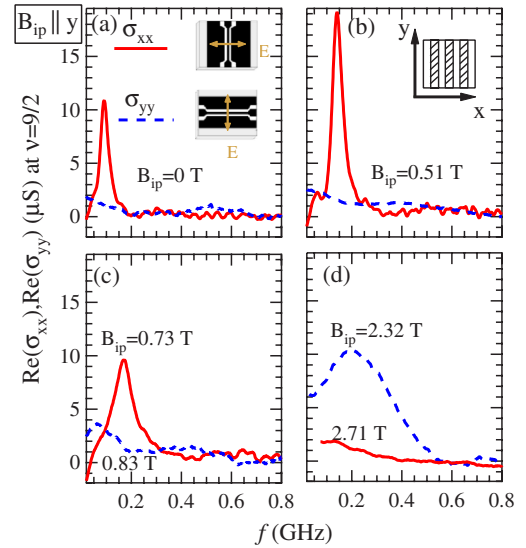


FIG. 1 (color online). Frequency spectra of real conductivities  $\text{Re}(\sigma_{xx})$  (solid lines) and  $\text{Re}(\sigma_{yy})$  (dashed lines), for  $B_{ip}$  along  $\hat{y}$  and increasing from (a) to (d).  $\sigma_{xx}$  is measured in sample 1, and  $\sigma_{yy}$  in sample 2. The inset shows a schematic of the microwave transmission line and the nominal stripe orientation at zero  $B_{ip}$ .

$B_{ip} = 0$ , taken from the same samples and cooldowns used for  $B_{ip} > 0$  in the rest of Fig. 1; a 90 MHz resonance is present in the spectrum of  $\text{Re}(\sigma_{xx})$ , for which  $E_{rf}$  is polarized in the hard direction, but there is no resonance in  $\text{Re}(\sigma_{yy})$ , for which  $E_{rf}$  is polarized in the easy direction. Application of  $B_{ip} \approx 0.51 \text{ T}$ , as shown in Fig. 1(b), does not switch the axis on which the resonance is observed; the resonance remains visible only in  $\text{Re}(\sigma_{xx})$ , with the peak conductivity  $\sigma_{pk}$  and peak frequency  $f_{pk}$  increased. In Fig. 1(c), the  $\text{Re}(\sigma_{xx})$  resonance at  $B_{ip} = 0.73 \text{ T}$  is also well-developed with  $f_{pk}$  increased further but  $\sigma_{pk}$  reduced. Also in Fig. 1(c), at  $B_{ip} = 0.83 \text{ T}$ ,  $\text{Re}(\sigma_{yy})$  shows a weak, low frequency peak. Figure 1(d) shows that, at the larger  $B_{ip}$ 's of 2.32 and 2.71 T, the resonance in  $\text{Re}(\sigma_{xx})$  is absent, while there is a broad resonance in  $\text{Re}(\sigma_{yy})$ , indicating that switching of the polarization of the resonance has occurred.

Figure 2 shows conductivity spectra for  $B_{ip}$  applied along  $\hat{x}$ , perpendicular to the  $B_{ip} = 0$  stripe direction. Figure 2(a) shows  $B_{ip} = 0$  spectra for reference, again taken in the same cooldowns used to obtain the  $B_{ip} > 0$  data in that figure. The samples used to obtain the data in Fig. 2 were the same as those used in Fig. 1 but had to be remounted and cooled again to obtain the data in Fig. 2 (to turn them in the rotator). As expected for different cooldowns of the same samples, the spectra in Figs. 1(a) and 2(a) are in good agreement, with a resonance only in  $\text{Re}(\sigma_{xx})$ . Figures 2(b)–2(d) again show that  $B_{ip}$  switches the polarization axis of the resonance. The switching appears to be taking place at  $B_{ip} = 0.29 \text{ T}$ , for which spectra

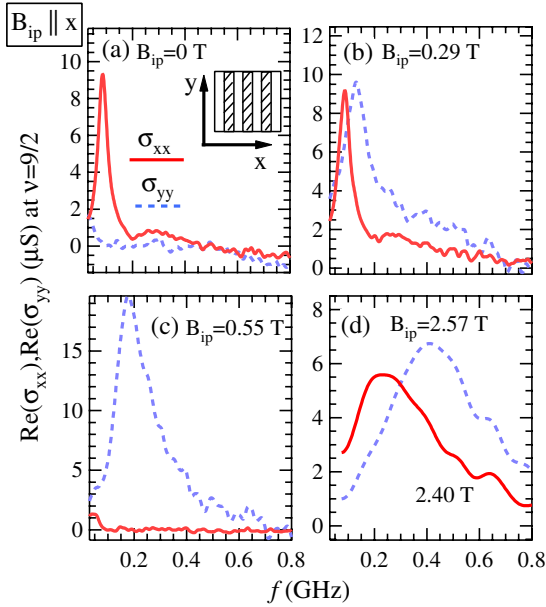


FIG. 2 (color online). Frequency spectra of real conductivities  $\text{Re}(\sigma_{xx})$  (solid lines) and  $\text{Re}(\sigma_{yy})$  (dashed lines), for increasing  $B_{ip}$  along  $\hat{x}$  from (a) to (d). The inset shows the nominal stripe orientation at zero  $B_{ip}$ .

in Fig. 2(b) show well-developed resonances both in  $\text{Re}(\sigma_{xx})$  and in  $\text{Re}(\sigma_{yy})$ . The switching is complete by  $B_{ip} = 0.55$  T: As seen in Fig. 2(c),  $\text{Re}(\sigma_{yy})$  shows a resonance at peak frequency 170 MHz, while  $\text{Re}(\sigma_{xx})$  shows none. Figure 2(d) presents data for the much larger  $B_{ip}$  around 2.5 T; resonances are again present in both directions but are qualitatively different from the lower  $B_{ip}$  resonances, with much larger linewidths and peak frequencies roughly twice of those in Fig. 2(b).

Figure 3 presents plots of the resonance peak conductivity  $\sigma_{pk}$  and frequency  $f_{pk}$  vs  $B_{ip}$ .  $\sigma_{pk}$  from both polarizations is shown in Fig. 3(a) for  $B_{ip}$  along  $\hat{x}$  and in Fig. 3(b) for  $B_{ip}$  along  $\hat{y}$ . In both panels there are distinct ranges of  $B_{ip}$  in which a resonance is present exclusively in  $\text{Re}(\sigma_{xx})$  or  $\text{Re}(\sigma_{yy})$ . Separating these ranges of one-polarization resonance, there are crossover ranges in which peaks can be observed in both  $\text{Re}(\sigma_{xx})$  or  $\text{Re}(\sigma_{yy})$ . This reinforces the description in which  $B_{ip}$ , applied on either axis can be thought of as switching the resonance from  $\text{Re}(\sigma_{xx})$  to  $\text{Re}(\sigma_{yy})$ . This switching of the polarization of the resonance is most naturally interpreted as a reorientation of the stripes, by analogy with the  $B_{ip}$ -induced switching of the hard and easy axes observed in dc transport studies [13–20]. Figure 3(c) shows  $f_{pk}$  vs  $B_{ip}$  for the two  $B_{ip}$  directions and sample axes, with each case having the same symbol as in Figs. 3(a) and 3(b). While all of the curves in Fig. 3(c) show  $f_{pk}$  increasing with  $B_{ip}$ , the rate of this increase is faster in the curves of  $\sigma_{xx}$  with  $B_{ip}$  along  $\hat{y}$  and of  $\sigma_{yy}$  with  $B_{ip}$  along  $\hat{x}$ . Hence, when  $B_{ip}$  is significant,

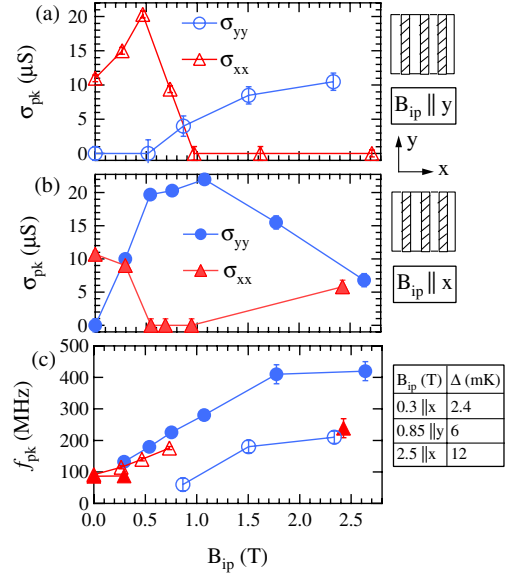


FIG. 3 (color online). (a) For in-plane field  $B_{ip}$  along  $\hat{x}$ , the resonance amplitudes in  $\text{Re}(\sigma_{xx})$  (solid triangles) and  $\text{Re}(\sigma_{yy})$  (solid circles), as functions of the magnitude of  $B_{ip}$ . (b) For  $B_{ip}$  along  $\hat{y}$ , the resonance amplitudes in  $\text{Re}(\sigma_{xx})$  (open triangles) and  $\text{Re}(\sigma_{yy})$  (open circles), as functions of  $B_{ip}$ . (c) The resonance peak frequencies vs  $B_{ip}$ , with the same symbols as in (a) and (b). The inset shows the nominal stripe orientation at zero  $B_{ip}$ . The table at right shows  $\Delta$ , the per-carrier pinning energy difference between stripes parallel and perpendicular to  $B_{ip}$ ; magnitudes and directions of  $B_{ip}$  at which  $\Delta$  is assessed appear in the left column.

these curves, for which  $E_{rf}$  polarization is perpendicular to  $B_{ip}$ , have larger  $f_{pk}$  than the curves with parallel  $E_{rf}$  and  $B_{ip}$ .

Of particular interest in interpreting the results are the narrow, transitional  $B_{ip}$  ranges in which the switching of the resonance polarization is taking place. In these ranges, resonances in  $\text{Re}(\sigma_{xx})$  and  $\text{Re}(\sigma_{yy})$  are both present for an applied  $B_{ip}$  magnitude and direction. The spectra in Fig. 2(b) are the most striking example of two well-developed resonances with different  $f_{pk}$  and linewidths present for the two polarizations, under the same conditions. Taking the presence of a resonance as an indicator of a region of stripes perpendicular to  $E_{rf}$ , the two resonances can be interpreted as arising from regions of different perpendicular stripe directions, coexisting at the transitional  $B_{ip}$ . Such coexistence would be consistent with energy minima at the orthogonal  $[110]$  and  $[1\bar{1}0]$  stripe orientations; such minima in stripe state energy vs orientation were proposed in Ref. [14], which reported stable or metastable states with these easy directions in dc transport.

The main result of this Letter is the dependence of  $f_{pk}$  on  $B_{ip}$ . In the context of weak pinning theories [22–24], this is a measure of the pinning energy—the average energy per carrier due to the potential of the pinning disorder. Since

the pinning energy is a disorder interaction, it is not explicitly present in the theories [31,32] that in the absence of disorder obtain the anisotropy energy  $E_A$  as a function of  $B_{ip}$  for a given sample vertical ( $z$ ) confinement. To affect  $f_{pk}$ ,  $B_{ip}$  must modify the effect of disorder, again by modifying the carrier wave function including  $z$  dependence. If the disorder relevant to pinning is due to interface roughness, as conjectured by Fertig [22] for the Wigner crystal,  $B_{ip}$  could increase pinning by increasing wave function amplitude at the quantum well interfaces. Such an effect can be inferred from the wave functions in a quantum well in higher Landau levels, in the presence of  $B_{ip}$ , as presented in Ref. [32].

The change in  $f_{pk}$  on applying  $B_{ip}$  is large enough to be comparable to the calculated  $E_A$  [13,31,32], implying that a disorder interaction, specifically pinning energy, plays an important role in determining the orientation (or other parameters) of the stripe state. For the transitional  $B_{ip}$ 's, at which resonances are present in both  $\sigma_{xx}$  and  $\sigma_{yy}$ , pinning energy anisotropy  $\Delta$  due to  $B_{ip}$  is directly obtained as the difference of  $f_{pk}$  measured with  $E_{rf}$  perpendicular and parallel to  $B_{ip}$ ; taking the resonances to be occurring when  $E_{rf}$  is polarized perpendicular to the stripes,  $\Delta = h[f_{pk}(\text{stripes} \parallel B_{ip}) - f_{pk}(\text{stripes} \perp B_{ip})]$ . The table next to Fig. 3(c) presents the  $\Delta$  and  $B_{ip}$  values. For comparison,  $E_A$ , calculated [13] for the same carrier density and quantum well thickness as in the present sample, is about 6 mK per carrier at  $B_{ip} = 0.8$  T. The pinning energy tends to stabilize the orientation of the stripes *parallel* to  $B_{ip}$  and so is competing with  $E_A$ , which for our sample favors the stripes perpendicular to  $B_{ip}$ . Interplay of this type may explain the complex switching behavior that we observed, with pinning energy driving the switching of the resonant polarization when  $B_{ip}$  is applied perpendicular to the original stripe direction. More generally, dependence of the carrier-disorder interaction on  $B_{ip}$  may explain some of the sample-dependent behavior of the stripe states that has been noted in dc transport experiments [15].

In summary, our studies of the stripe phase in  $B_{ip}$  indicate that disorder-carrier interaction in the stripe phase, as measured by  $f_{pk}$ , increases with  $B_{ip}$  and plays an important role in the symmetry breaking that determines the stripe orientation. The presence of resonances in both polarizations around the  $B_{ip}$  of the apparent switching of the stripe direction indicates there are likely coexisting regions of perpendicularly oriented stripes at the transition.

This work was supported by DOE Grants No. DEFG21-98-ER45683 at Princeton and No. DE-FG02-05-ER46212

at NHMFL. NHMFL is supported by NSF Cooperative Agreement No. DMR-0084173, the State of Florida, and the DOE.

- 
- [1] M. P. Lilly *et al.*, Phys. Rev. Lett. **82**, 394 (1999).
  - [2] R. R. Du *et al.*, Solid State Commun. **109**, 389 (1999).
  - [3] M. M. Fogler, A. A. Koulakov, and B. I. Shklovskii, Phys. Rev. B **54**, 1853 (1996).
  - [4] R. Moessner and J. T. Chalker, Phys. Rev. B **54**, 5006 (1996).
  - [5] A. H. MacDonald and M. P. A. Fisher, Phys. Rev. B **61**, 5724 (2000).
  - [6] E. Fradkin and S. A. Kivelson, Phys. Rev. B **59**, 8065 (1999).
  - [7] Q. M. Doan and E. Manousakis, Phys. Rev. B **75**, 195433 (2007); **78**, 075314 (2008).
  - [8] H. Yi, H. A. Fertig, and R. Côté, Phys. Rev. Lett. **85**, 4156 (2000).
  - [9] M.-R. Li *et al.*, Phys. Rev. Lett. **92**, 186804 (2004); Phys. Rev. B **71**, 155312 (2005).
  - [10] A. M. Ettouhami *et al.*, Phys. Rev. Lett. **96**, 196802 (2006).
  - [11] K. Tsuda, N. Maeda, and K. Ishikawa, Phys. Rev. B **76**, 045334 (2007).
  - [12] R. L. Willett *et al.*, Phys. Rev. Lett. **87**, 126803 (2001).
  - [13] K. B. Cooper *et al.*, Solid State Commun. **119**, 89 (2001).
  - [14] K. B. Cooper *et al.*, Phys. Rev. Lett. **92**, 026806 (2004).
  - [15] J. Zhu *et al.*, Phys. Rev. Lett. **88**, 116803 (2002).
  - [16] M. P. Lilly *et al.*, Phys. Rev. Lett. **83**, 824 (1999).
  - [17] W. Pan *et al.*, Phys. Rev. Lett. **83**, 820 (1999).
  - [18] K. B. Cooper *et al.*, Phys. Rev. B **65**, 241313(R) (2002).
  - [19] H. Takado *et al.*, J. Phys. Soc. Jpn. **76**, 074712 (2007).
  - [20] W. Pan *et al.*, Phys. Rev. Lett. **85**, 3257 (2000).
  - [21] G. Sambandamurthy *et al.*, Phys. Rev. Lett. **100**, 256801 (2008).
  - [22] H. A. Fertig, Phys. Rev. B **59**, 2120 (1999).
  - [23] M. M. Fogler and D. A. Huse, Phys. Rev. B **62**, 7553 (2000).
  - [24] R. Chitra, T. Giamarchi, and P. Le Doussal, Phys. Rev. Lett. **80**, 3827 (1998); Phys. Rev. B **65**, 035312 (2001).
  - [25] P. D. Ye *et al.*, Phys. Rev. Lett. **89**, 176802 (2002).
  - [26] M. Shayegan *et al.*, *Perspectives in Quantum Hall Effects* (Wiley Interscience, New York, 1997), Chap. 9.
  - [27] Y. Chen *et al.*, Phys. Rev. Lett. **91**, 016801 (2003).
  - [28] R. M. Lewis *et al.*, Phys. Rev. Lett. **89**, 136804 (2002).
  - [29] J. Göres *et al.*, Phys. Rev. Lett. **99**, 246402 (2007).
  - [30] E. Orignac and R. Chitra, Europhys. Lett. **63**, 440 (2003).
  - [31] T. Jungwirth, A. H. MacDonald, L. Smrčka, and S. M. Girvin, Phys. Rev. B **60**, 15574 (1999).
  - [32] T. D. Stanescu, I. Martin, and P. Phillips, Phys. Rev. Lett. **84**, 1288 (2000).